

Rate Constants and Thermodynamic Parameters of Rotation of Axial Ligands in a Bisligated Ferric Tetramesitylporphyrinate Complex Measured from the Temperature Dependence of ^1H Transverse Relaxation Rates

Konstantin I. Momot¹ and F. Ann Walker*

Department of Chemistry, University of Arizona, Tucson, Arizona 85721

Received: July 7, 1998; In Final Form: October 5, 1998

The rate constant of the four-site cyclic chemical exchange between pyrrole protons in tetramesitylporphyrinatoiron(III)bis(2-methylimidazole) has been measured in the temperature range 236–255 K from ^1H transverse relaxation times (T_2) observed at the 500 MHz field strength. The values of the rate constant were obtained through the simulation of the observed T_2 's under the assumption that their values are dominated by the rate of the chemical exchange. The measurement of the exchange rate constant was also attempted at a lower temperature (230 K), but the use of extrapolated intrinsic T_2 's at that temperature introduces a significant error into the simulated rate constant. The thermodynamic activation parameters of the cyclic exchange were determined as $\Delta H^\ddagger = 48 \pm 1$ kJ/mol and $\Delta S^\ddagger = -10 \pm 6$ J/K·mol. The value of k varied from 30 to 270 s^{-1} in the temperature range 236–255 K. The near-zero exchange activation entropy is consistent with two previous studies but contradicts another study based on saturation-transfer measurements previously carried out by the authors of this work. A comparison of all available studies shows that the saturation-transfer experiments overestimate the value of the exchange rate constant by up to a factor of 2. It is shown that equilibrium with the high-spin form of the porphyrin complex does not affect the observed T_2 's in the temperature range used in this study but may do so at temperatures above 270 K. It is also shown that neither the linearity of the Curie plot nor the behavior of the T_1 versus temperature plot should be considered indicators of the absence of the low-spin \rightleftharpoons high-spin equilibrium.

Introduction

Tetraphenylporphyrin complexes with 2,6-disubstituted phenyl rings and bulky axial ligands are unique among bisligated metalloporphyrins in that the rotation of axial ligands in such complexes can be quantitatively studied by ^1H NMR over a relatively wide range of temperatures. Tetramesitylporphyrinatoiron(III)bis(2-methylimidazole), [(TMP)Fe(2-MeImH)₂]⁺, is one such complex; the rate of rotation of its 2-methylimidazole ligands has been measured in the temperature range of 200–245 K by various ^1H NMR methods.^{2–6} Below 200 K, the ligands are effectively frozen in mutually perpendicular orientations, bisecting the porphyrin ring nitrogens. Frozen unsymmetrical axial ligands, along with the ruffling of the porphyrin core,⁷ introduce asymmetry into this otherwise symmetric complex. This results in four distinct signals from the pyrrole protons being observed in the ^1H NMR spectrum. Above 200 K, the axial ligands slowly rotate, inducing a four-site cyclic chemical exchange between pyrrole protons. As the temperature is increased further (273 K at 500 MHz and 265 K at 300 MHz field strength), the exchange becomes fast on the NMR time scale and all pyrrole protons become equivalent in the NMR spectrum.

Rotation of axial ligands in [(TMP)Fe(2-MeImH)₂]⁺ has been studied by total line shape simulation analysis of ^1H spectra,^{5,6} 2D exchange spectroscopy (EXSY),^{2,3} ^1H saturation-transfer (ST) spectroscopy,⁴ and molecular mechanics.⁴ In NMR studies, the rate of axial ligand rotation is identified as the rate constant of the cyclic chemical exchange between pyrrole or *o*-methyl protons induced by such rotation.^{2–4} For this reason, the terms “the rate of cyclic exchange” and “the rate of ligand rotation” will be used interchangeably in this paper. Thermodynamic activation parameters of the cyclic exchange have been determined from the temperature dependence of the rate constant

TABLE 1: Thermodynamic Parameters of the Cyclic Exchange from Various Measurements

method	ΔH^\ddagger , kJ/mol	std er	ΔS^\ddagger , J/K·mol	std er
NMR (EXSY) ^{a,b}	51	3	3	15
NMR (DNMR line shape) ^{b,c}	54	2	16	7
NMR (saturation-transfer) ^{b,d}	59	1	41	5
T_2 simulation ^{b,e}	48	1	-10	6
MM2 ^{d,f}	48		not measured	

^a Reference 2. ^b [(TMP)Fe(2-MeImH)₂]⁺. ^c Reference 5. ^d Reference 4. ^e This work. ^f [(TMP)Fe(1,2-Me₂Im)₂]⁺.

and are summarized in Table 1. The values of the ΔH^\ddagger of rotation determined in the different studies are slightly different, although comparable (ca. 50 kJ/mol). However, the values of the ΔS^\ddagger of rotation are qualitatively different between refs 2,3 and 5,6 (where the entropy is effectively 0, considering the margin of error) and ref 4 (where the entropy has a significantly positive value).

In the current study, we have undertaken an NMR measurement of the rate of axial ligand rotation and rotational ΔH^\ddagger , ΔS^\ddagger , using the T_2 's of the pyrrole protons. It has been found⁸ that the temperature dependence of transverse relaxation rates of pyrrole protons in [(TMP)Fe(2-MeImH)₂]⁺ is bimodal in that the T_2 's increase with temperature at low temperatures and decrease at high temperatures preceding the collapse of the four-peak pyrrole proton pattern. This behavior is compatible with the hypothesis that at low temperatures the T_2 's of the pyrrole protons are the intrinsic T_2 's, which increase with temperature, whereas at the high temperatures the T_2 values are significantly shortened by exchange.⁸

The decay of longitudinal or transverse magnetization of spins undergoing chemical exchange is in general described by multiple relaxation times.⁹ However, a single effective T_2 can

be introduced in the least-squares sense if the deviations from the single-exponential behavior are numerically small and uniform throughout the range of the decay time values. Whether this is the case can be verified by the linearity of the semilogarithmic intensity plot versus defocusing time.

The observed transverse relaxation rate, $R_{2\text{obs}}$, is a function of the intrinsic chemical shifts $\{\omega^0\}$ and the intrinsic relaxation rates $\{R_1^0, R_2^0\}$ of all spins in an exchange pattern, as well as the exchange rate constant(s)

$$R_{2\text{obs}} = R_2^0 + R_{\text{exch}}(k, \{\omega^0\}, \{R_1^0\}, \{R_2^0\}) \quad (1)$$

For the case of a two-site exchange, $T_{2\text{obs}}$ can be found analytically.¹⁰ For a larger number of sites, the function R in eq 1 can only be defined numerically, because the analytical formulas become prohibitively complex. When intrinsic chemical shifts and intrinsic relaxation times are known, they can be regarded as fixed parameters, and therefore, function R in eq 1 will contain only exchange rate constant(s) as variable(s).

This formalism is similar to that of the total line shape simulation analysis (TLSA).^{5,6} However, the two approaches are not identical. The approach used in this study simulates the spectrum as a function of the defocusing/refocusing time in the Hahn spin-echo experiment. The effective $T_{2\text{obs}}$ for each peak is obtained from the least-squares fit of intensity versus decay time. In the TLSA approach, the effective $T_{2\text{obs}}$ of a peak is determined from its line width in the simulated single-pulse ($\pi/2$) spectrum. This imposes the requirement of very good shimming when the experimental spectra are acquired. Additionally, the criteria of the fit quality are not defined as clearly as when a single parameter (T_2) is simulated, because different parts of the spectrum carry different weights when fit quality is determined.

As mentioned above, effective transverse relaxation times were simulated in this work by reproducing the behavior of proton magnetization during the Hahn spin-echo experiment.¹¹ Because the magnitude of scalar couplings of pyrrole protons is significantly smaller than that of their line width, the Bloch equations provide an adequate tool for simulating the behavior of proton magnetization. In the absence of a radio frequency (rf) pulse, the behavior of magnetization is described by the Bloch equations modified to take exchange into account:

$$\frac{d\overline{M}_z}{dt} = \hat{R}_1(\overline{M}_z - \overline{M}_z^\infty) + \hat{K}\overline{M}_z \quad (2)$$

$$\frac{d\overline{M}_+}{dt} = -i\hat{\Omega}\overline{M}_+ + \hat{R}_2\overline{M}_+ + \hat{K}\overline{M}_+ \quad (3)$$

For the case of the TMP complex which exhibits a four-site cyclic exchange, the terms in eqs 2 and 3 are given by

$$\mathbf{M}_z = \begin{pmatrix} M_{zA} \\ M_{zB} \\ M_{zC} \\ M_{zD} \end{pmatrix} \quad \mathbf{M}_z^\infty = \begin{pmatrix} M_{zA}^\infty \\ M_{zB}^\infty \\ M_{zC}^\infty \\ M_{zD}^\infty \end{pmatrix} \quad (4)$$

$$\hat{K} = \begin{pmatrix} -2k & k & 0 & k \\ k & -2k & k & 0 \\ 0 & k & -2k & k \\ k & 0 & k & -2k \end{pmatrix} \quad (5)$$

and \hat{R}_1 , \hat{R}_2 , and $\hat{\Omega}$ are diagonal matrices which contain respective

relaxation times or precession frequencies of the four spins. Equations 2 and 3 describe the behavior of magnetization during evolution delays and the acquisition period. During the latter, free induction decay (FID) can be generated by sampling the complex vector of the net transverse magnetization at equidistant times. The spectrum is obtained by applying a Fourier transformation (FT) to the FID. Because there are no hardware factors involved in the simulations, there is no need for phasing or baseline correction. In simulations of Hahn spin-echo experiments, there also is no need for phase cycling.

Evolution of magnetization during rf pulses can be simulated by application of the appropriate rotation operators, which are defined by the axis and the angle of rotation. Combining appropriate evolution delays, pulses, and acquisition (with phase cycling, if necessary) allows one to simulate entire NMR experiments. Mathematica software¹² provides a convenient interface for such simulations. Previously, packages implementing the product operator method have been described in the literature.^{13,14} We have created a Mathematica code for simulating NMR experiments using the Bloch equations. This approach allows the simulation of the inversion recovery and Hahn spin-echo experiments, producing a series of spectra simulated at different delay times. The relevant relaxation times can be determined from these spectra as if they were recorded experimentally.

In this study, we will use simulation of the experimentally observed pyrrole proton T_2 's in $[(\text{TMP})\text{Fe}(\text{2-MeImH})_2]^+$ to demonstrate that the presence of cyclic chemical exchange quantitatively explains their bimodal behavior.⁸ The rate of rotation of axial ligands can be measured from the temperature dependence of the T_2 's as the rate constant of chemical exchange induced by such rotation. We will also compare this approach to the others that have been used to determine the rate of axial ligand rotation in the complex²⁻⁵ and show that the saturation-transfer method³ significantly overestimates the rate.

Experimental Section

1. Materials. Synthesis of the iron(III) tetramesitylporphyrinates utilized for this study has been described elsewhere.¹⁵ Degassed NMR samples of the bis(2-MeImH)iron(III) tetramesitylporphyrinate perchlorate and bis(1,2-Me₂Im)iron(III) tetramesitylporphyrinate perchlorate complexes were prepared as described previously.^{4,8} Chemical shifts and longitudinal relaxation times of pyrrole protons in $[(\text{TMP})\text{Fe}(\text{2-MeImH})_2]^+$ were previously measured at the 500 MHz field strength.⁸ Spectra of bis(1,2-Me₂Im)iron(III) tetramesitylporphyrinate perchlorate, $[(\text{TMP})\text{Fe}(\text{1,2-Me}_2\text{Im})_2]^+$, were obtained in this study using identical procedures.⁸

2. T_2 Relaxation Measurements. Transverse relaxation times of pyrrole protons in $[(\text{TMP})\text{Fe}(\text{2-MeImH})_2]^+$ were remeasured at the 500 MHz field strength in this work with improved temperature calibration. The T_2 's were recorded using the Hahn spin-echo pulse sequence¹¹ modified for the operation in inverse mode: spectral width, 35 kHz; acquisition time, 0.2 s; recycling delay, 1 s; 2 dummy scans and 64–128 transients; and data size, 8 K complex points. The highest available decoupling power was used to produce the hard pulses ($\pi/2$ pulse length, 7 μs). The number of spectra in each temperature series was between 10 and 20, depending on the temperature and expected value of the relaxation time. In the series containing 20 spectra, the defocusing/refocusing time varied between 0.1 and 20 ms. Processing using Felix 95¹⁶ included FID drift offset correction, Bruker FT, phasing, and seventh-order polynomial baseline correction. Pyrrole proton signals

were integrated to the corrected baseline level, and the integrals were used to obtain the values of T_2 's by the linear least-squares fitting of the decay data in semilogarithmic coordinates

$$\sum_i [\ln(I_i) - a_0 - b \times 2\tau_i]^2 = \min \quad (6)$$

where b has the meaning of T_2^{-1} . The applicability of a single T_2 was verified for at least one exchanging peak at each temperature through semilogarithmic intensity plots of experimental data. This also ensured that the measured relaxation times were not affected by diffusion. In all cases, the deviations from linearity were very small and did not have systematic character.

3. Simulation Parameters. The observed chemical shift values were used as the intrinsic shifts.⁸ The shifts were referenced so that their Larmor frequencies were between 0 and 8000 Hz. Observed T_1 's were used as the intrinsic T_1 's. T_2 's of pyrrole protons of the studied complex have been measured in this work in the temperature range of 198–255 K, as described above.

Originally, it was intended that low-temperature (198–224 K) T_2 data be used to extrapolate the intrinsic relaxation times, T_{20} . The values of the intrinsic T_2 's were extrapolated from the range of 198–224 K using the functional form

$$\ln T_2 = A/T + B \quad (7)$$

where A and B are constant for a given proton. It was found that at 230 K the extrapolation error is comparable to the value of the simulated exchange rate constant and that at all temperatures the error was 10–25% of the extrapolated T_2 's. This margin of error required that the 230 K data be excluded from the determination of the exchange activation parameters and that the extrapolation be used only when $T_{2\text{obs}}^{-1} \gg T_{20}^{-1}$.

4. Simulation Procedure. Simulations of the experimental T_2 's consisted of three logical parts combined into a single program. The first part numerically simulated spectra of a four-spin system with chemical exchange as a function of the defocusing delay τ . The second part determined the effective simulated T_2 for each peak in the spectrum using peak intensities at two different values of τ . The third part was the search procedure that varied the rate constant of the cyclic exchange, k , to reproduce the experimental $T_{2\text{obs}}$ of the target peak.

Hahn spin-echo experiments were simulated by applying appropriate pulses and evolution periods to the four spins, "acquiring" the FID under evolution operators given by eqs 2 and 3, and applying FT to it. The procedure was repeated for another recovery/refocusing time, and peak integrals were used to obtain the observed relaxation times

$$T_{2\text{obs}} = \frac{2(\tau_2 - \tau_1)}{\ln(I_1/I_2)} \quad (8)$$

where $T_{2\text{obs}}$ is the observed T_2 value of the peak whose T_2 is being simulated, and I_i is its intensity at the defocusing time τ_i . Defocusing times τ_1 and τ_2 were chosen so that the ratio of I_1/I_2 is between 2 and 3.

For several simulated situations, the linearity of the simulated magnetization decays was verified. In these cases, the simulation procedure was performed at 10–20 different values of the defocusing time rather than 2. The effective transverse relaxation rates in these cases were determined by least-squares fitting using eq 6. For all verified cases, the deviation of the individual points from the fit line was marginal and the difference between the $T_{2\text{obs}}$ values determined by eqs 6 and 8 did not exceed 1%.

Each individual simulation reproduced the experimentally observed T_2 value of a single peak in the spectrum. Therefore, four simulations were performed for each temperature, and four values of the exchange rate constant were obtained.

The search for the k value reproducing the target $T_{2\text{obs}}$ was implemented using the *Regula Falsi*.¹⁷ Two starting points were required by the search procedure. These were chosen as $k = 0$ ($T_{2\text{obs}} = T_{20}$) and a value of k obtained from previous measurements.^{2–6} In some cases, the originally chosen starting points failed to generate a converging search, and the second starting point had to be adjusted. The search was repeated until the deviation of the simulated T_2 from the target values (experimental $T_{2\text{obs}}$) was within 0.005%.

5. Exchange Activation Parameters and Error Determination. The values of the activation enthalpy and entropy of the cyclic exchange (ΔH^\ddagger and ΔS^\ddagger) were determined by linear regression of the points of the Eyring plot, $\ln(kh/k_B T)$ versus $1/T$. Data points acquired at the four highest temperatures (236–255 K) were used for the regression. Although the exchange rate constant was also determined at 230 K, these points were excluded from the ΔH^\ddagger and ΔS^\ddagger determinations, for reasons discussed below.

The error of the experimental T_2 's was determined in the least-squares fit procedure used to determine the T_2 's (eq 6). It typically did not exceed 1 ms. The accuracy of the temperature calibration is estimated as ± 0.5 K. The errors of the exchange rate constant, k , at different temperatures were not determined but can be estimated by comparing the four values of k at a given temperature.

The errors of the thermodynamic activation parameters of the cyclic exchange were determined during the linear regression procedure that was used to produce the values of ΔH^\ddagger and ΔS^\ddagger . Because this method accounts for only the statistical deviation of the data points and does not explicitly consider instrumental instabilities, the actual errors of the ΔH^\ddagger and the ΔS^\ddagger are likely to be somewhat greater than the values given in Table 1. An analysis incorporating instrumental temperature instabilities into the ΔH^\ddagger and ΔS^\ddagger errors was performed using the approach given by Bevington.¹⁸ This analysis showed that the temperature instabilities lead to minor contributions to the errors that are significantly smaller than the statistical deviation errors determined in the LSF procedure.

Results and Discussion

1. Measurement of the Rate of the Cyclic Exchange from Proton T_2 . Simulation of exchange-modified NMR spectra is an effective way of measuring the rate constant of slow to intermediate (on the NMR time scale) chemical exchange reactions. The formalism for this approach for the case of CW (continuous wave) NMR spectroscopy is well described in Slichter's monograph.¹⁹ It is easily extended to FT NMR spectroscopy by adding the relevant exchange terms to the Bloch equations, which are adequate for the treatment of $S = 1/2$ spins that are not coupled to each other.²⁰ Analytical expressions are easily obtained for the two-site case^{19,21,22} and are significantly more complex for the general three-site⁹ and higher cases.^{23,24}

Since the method was first introduced, an extremely large number of applied works have appeared. Therefore, only a few of the most representative papers^{25–30} and reviews^{9,31,32} are cited here to illustrate the use of the approach for the determination of rate constants and activation parameters of chemical exchange.

In this work, exchange-modified pyrrole proton T_2 's in [(TMP)Fe(2-MeImH)₂]⁺ are simulated in order to obtain the

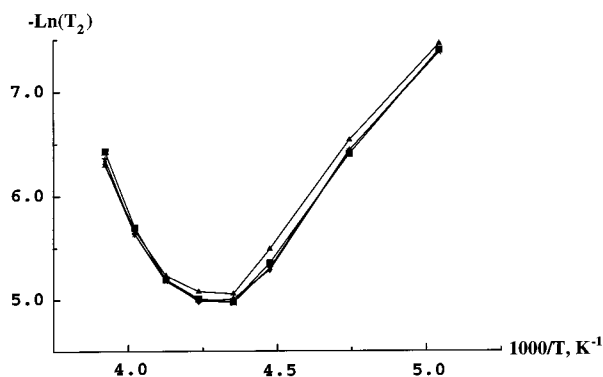


Figure 1. Temperature dependence of the pyrrole T_2 's of $[(\text{TMP})\text{Fe}(\text{2-MeImH})_2]^+$. The values of the exchange activation parameters were obtained using the four leftmost points. The three rightmost points were used to obtain the intrinsic T_{20} 's by extrapolation.

rate constant of the exchange. The observed T_2 's were obtained as described previously.⁸ The rates of exchange were obtained by means of numerical simulation of the T_2 's under four-site cyclic chemical exchange as described in the Experimental Section. The temperature dependence of the observed T_2 's is presented in Figure 1.

At 190 K, $[(\text{TMP})\text{Fe}(\text{2-MeImH})_2]^+$ shows four NMR signals from pyrrole protons because of the fact that its unsymmetrical axial ligands are frozen in a definite orientation.^{33,34} At 200–270 K, the four peaks undergo cyclic chemical exchange induced by the synchronous rotation of axial ligands that is slow to intermediate on the NMR time scale, depending on the temperature and the field strength. The peaks eventually collapse into one peak (273 K at 500 MHz and 265 K at 300 MHz field strength). As a result, the temperature dependence of transverse relaxation times (T_2 's) of the pyrrole protons exhibits a bimodal behavior, as shown in Figure 1. Below 225 K ($1/T = 0.0044 \text{ K}^{-1}$) at 500 MHz, the transverse relaxation times of the pyrrole protons are essentially the intrinsic T_2 's governed by the distribution of the spin density in the molecule. In this region, the plot of $\ln(T_2)$ against $1/T$ is linear.^{35,36}

Above 225 K ($1/T = 0.0044 \text{ K}^{-1}$, Figure 1), the T_2 's of the pyrrole protons are modified by cyclic chemical exchange. If the intrinsic relaxation rates and the chemical shifts are known, the rate constant of the exchange can be obtained easily and accurately from the values of the modified T_2 's. Further, the exchange rate constant can be accurately determined even if the intrinsic T_{20} 's are not known exactly but are much smaller than the observed T_2 's.

In addition to the cyclic exchange, six-coordinate ferric tetraphenylporphyrinates can also exhibit chemical exchange of imidazole ligands between their free and bound states.⁸ The latter process has been shown to proceed through a 5-coordinate high-spin intermediate,^{36,37} which can shorten the T_2 's of the pyrrole–H resonances of the low-spin complex. If the low-spin–high-spin exchange is present in $[(\text{TMP})\text{Fe}(\text{2-MeImH})_2]^+$, the reliable determination of the cyclic exchange rate constant would require that either the two processes be deconvoluted or the cyclic exchange be studied in the temperature range where the low-spin–high-spin exchange does not occur.

In the studied bis(2-methylimidazole) complex, an accurate sensor of the presence or absence of the low-spin–high-spin exchange is provided by the NMR signal of the 1-methyl protons of the analogous complex with 1,2-dimethylimidazole ligands,³⁶ hereafter referred to as the control peak. The location of the control peak depends on the temperature and varies between +10 and +30 ppm. Up to 288 K, the peak is well-resolved

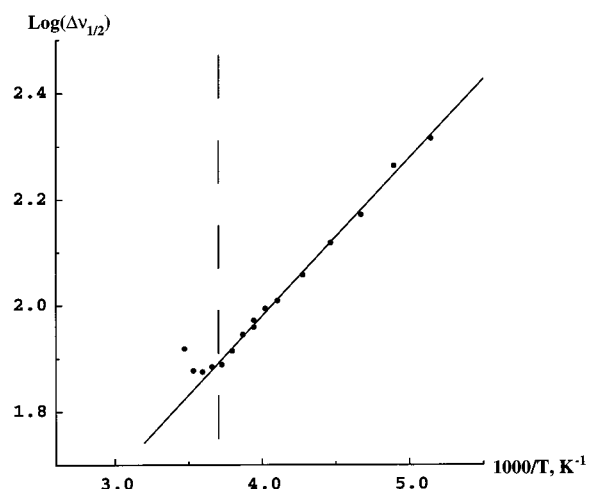


Figure 2. Plot of $-\log(\Delta\nu_{1/2})$ vs $1/T$ for the 1-methyl peak of the coordinated imidazole in $[(\text{TMP})\text{Fe}(\text{1,2-Me}_2\text{Im})_2]^+$ (control peak). When the ligand on/off exchange is absent (rate constant \ll line width), the logarithm of the line width of the peak varies linearly with $1/T$. The plot is nonlinear when the on/off exchange is present (i.e., left of the vertical line). This behavior is unaffected by the four-site cyclic exchange. The line width of the control peak is similar to those of the pyrrole peaks participating in the cyclic exchange. Therefore, the plot identifies the temperature regions in which the on/off exchange does and does not affect the peaks participating in the four-site exchange.

from all other peaks in the spectrum. Its T_2 strongly depends on the temperature and is comparable to those of the pyrrole protons in both this complex and $[(\text{TMP})\text{Fe}(\text{2-MeImH})_2]^+$. The imidazole binding constants in the two complexes are also similar,¹⁵ which suggests that the on/off rates are also similar. The T_2 of the control peak is not affected by the cyclic exchange, but exchange with the free ligand shortens it. In the absence of exchange between bound and free ligand, the plot of the logarithm of the line width of the control peak, $\log(\Delta\nu_{1/2})$, against inverse temperature, $1/T$, should be linear. In the presence of the exchange, the plot will exhibit nonlinear behavior corresponding to exchange broadening.

The plot of $\log(\Delta\nu_{1/2})$ of the control peak versus $1/T$ is shown in Figure 2 for the temperature region 194–288 K. The dashed vertical line in Figure 2 separates the region where the exchange is immeasurable from the region where the exchange can be measured, even if with poor accuracy. The position of the line corresponds to 270 K. Therefore, the ligand on/off exchange is negligible in the region 230–255 K, and the T_2 's of the pyrrole protons in that temperature region can be used for the determination of the cyclic exchange rate without the need to correct them for the rate of the low-spin–high-spin exchange. However, above 270 K, the ligand on/off exchange is not negligible.

The values of the observed $T_{2\text{obs}}$ are very sensitive to the rates of the exchange processes. Exchange noticeably modifies transverse relaxation rates even when no modification of the T_1 's or chemical shifts can be observed.⁸ Therefore, the temperature dependence of the pyrrole T_2 's should provide an accurate measure of the rate of the cyclic exchange, provided that the effects of the low-spin–high-spin exchange are excluded.

The rate constant of the four-site cyclic exchange in the temperature range 230–255 K was obtained by the simulation of the observed T_2 of each pyrrole signal. At each studied temperature, four values of the rate constant of the cyclic exchange have been obtained, one from each peak. This approach recognizes the fact that the experimentally observed T_2 's are measured with finite accuracy, and therefore, simulation

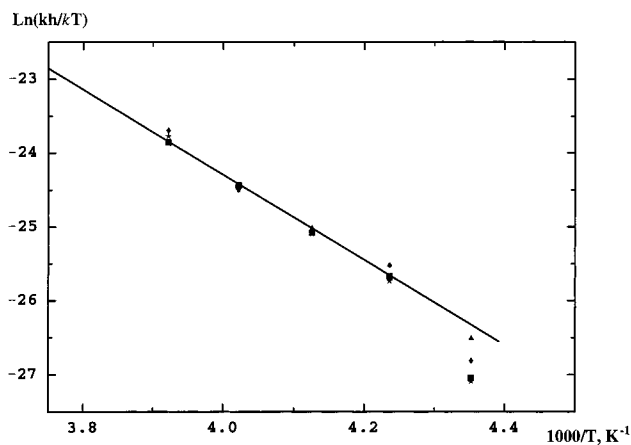


Figure 3. Eyring plot of the simulated rate constants in [(TMP)Fe(2-MeImH)₂]⁺. The negative of the slope of the regression line is the activation enthalpy of the exchange, and the intercept with the y axis is the activation entropy (both in units of *R*). Four points were obtained for each of the five temperatures used in the simulations: one point for each pyrrole proton. The lowest temperature data (230 K) were excluded from the determination of the activation parameters.

TABLE 2: Rate Constants of the Cyclic Exchange Determined from Pyrrole Transverse Relaxation Times

<i>T</i> , K	rate, s ⁻¹ , measured from			
	peak 1	peak 2	peak 3	peak 4
229.8	10.8	8.2	8.6	14.7
236.1	40.6	32.8	34.9	40.7
242.4	65.1	63.9	64.7	68.8
248.7	120.0	119.0	126.0	126.0
255.0	272.0	251.0	231.0	230.0

of the *T*₂'s of different peaks may yield different exchange rate constants at the same temperature. In addition, simulation of the *T*₂'s of individual peaks yields four values of the rate constant at any given temperature instead of just one value, as given by the two other approaches. As a result, the thermodynamic analysis of the exchange data is less sensitive to any single point.

The simulation procedure required the knowledge of the observed *T*₂ of the simulated peak (the most critical parameter), all four intrinsic *T*₂'s (not critical, except at 230 K), and the intrinsic chemical shifts and *T*₁'s of all four peaks in the exchange pattern (least critical parameters). The results are presented in Table 2 and Figure 3. In Figure 3, a regression line to the data points is also shown, to determine the thermodynamic activation parameters for the exchange. Values of $\Delta H^\ddagger = 48 \pm 1$ kJ/mol and $\Delta S^\ddagger = -10 \pm 6$ J/K·mol were obtained from the data in Table 2.

The lowest (rightmost in Figure 3) temperature data were excluded from the linear regression for the following reason. The rate of exchange is roughly proportional to the difference between the observed and intrinsic relaxation rates. When this difference is similar to the observed relaxation rate, the error of the determination of the exchange rate constant is much smaller than the constant itself. When the observed and intrinsic relaxation rates are almost the same, as is the case at the excluded temperature, the error of the exchange rate constant determination is similar to the value of the rate constant. As can be seen from Table 2, the values of the exchange rate constant determined at the excluded temperature vary between 8 and 15 s⁻¹, i.e., by almost a factor of 2. In a logarithmic plot such as the one in Figure 3, this transforms into a significant discrepancy between the individual data points that makes the regression results very sensitive to the inclusion/exclusion of a

single point. The value of *k* simulated at 230 K was also found to be sensitive to the method of extrapolation of the intrinsic *T*₂₀'s. For all other temperatures, the extrapolation method and the values of the intrinsic *T*₂'s were found to have little effect on the simulated values of the exchange rate constant.

Neither the intrinsic *T*₁'s nor the intrinsic chemical shifts of the pyrrole protons were found to have a significant effect on the results of the simulations or the derived thermodynamic activation parameters.

2. Comparison of Activation Parameters from Different Experiments. The thermodynamic activation parameters of chemical exchange (ΔH^\ddagger , ΔS^\ddagger) are obtained by means of linear regression of data points of the Eyring plot. ΔH^\ddagger in units of *R* is the slope of the regression line, taken with the negative sign, and ΔS^\ddagger in units of *R* is the intercept of the regression line. The error of the determination of the intercept and the slope in the linear regression is inversely proportional to the spread of values of the independent variable (*x*).¹⁸ Therefore, provided that the reliability of measurements is uniform throughout the range of *x*, a wider temperature interval provides for an intrinsically more accurate measurement of ΔH^\ddagger and ΔS^\ddagger .

With regard to the rotation of axial ligands in [(TMP)Fe(2-MeImH)₂]⁺, this premise is complicated by a number of factors. The first factor is the presence of the ligand on/off exchange at high temperatures that was discussed previously⁸ and in the preceding section of this paper. Even if it can be deconvoluted from the cyclic exchange, the error of the measurement of the second rate constant propagates into the measurement of the cyclic exchange.

The second factor limits the applicability of those methods that rely on the magnetization transfer (nuclear Overhauser enhancement spectroscopy/EXSY or nuclear Overhauser enhancement (NOE)/ST difference). When the exchange is not very slow, all peaks in the magnetization transfer spectrum have similar intensities. However, a significant difference in the intensities of the diagonal and off-diagonal peaks is required for the reliable determination of the exchange rate constant.^{2-4,38}

At temperatures below 200 K at 500 MHz, the cyclic exchange in the studied complex is practically nonobservable on the NMR time scale.⁴ This is manifested by the extremely low intensities of NOE (or ST) peaks and the very long experimental times required to obtain reasonable signal-to-noise ratios.

Therefore, the temperature interval over which the rate of the cyclic exchange can be reliably measured is intrinsically limited on both sides. As a result, the width of the temperature interval in this and all other available studies of [(TMP)Fe(2-MeImH)₂]⁺ is comparable and is within 40 K. This intrinsic limitation leads to the challenging experimental problem of obtaining the individual measurements with accuracy sufficient to avoid the infamous “ ΔH^\ddagger versus ΔS^\ddagger ” artifact.²⁶

One of the requirements that should be used to ensure that the “ ΔH^\ddagger versus ΔS^\ddagger ” artifact is not present is the exclusion of those experimental points that disproportionately influence the resulting values of the ΔH^\ddagger and ΔS^\ddagger . Although no such points were present in the saturation-transfer data (ref 4), the lowest temperature points of the *T*₂ data of this work had to be excluded.

Another requirement is the avoidance of the “temperature-proportional” temperature miscalibration. If the high temperatures are miscalibrated with a positive systematic error and the low temperatures are miscalibrated with a negative systematic error, both ΔH^\ddagger and ΔS^\ddagger are underestimated. It is believed that both requirements have been well followed in the ST,⁴ as well

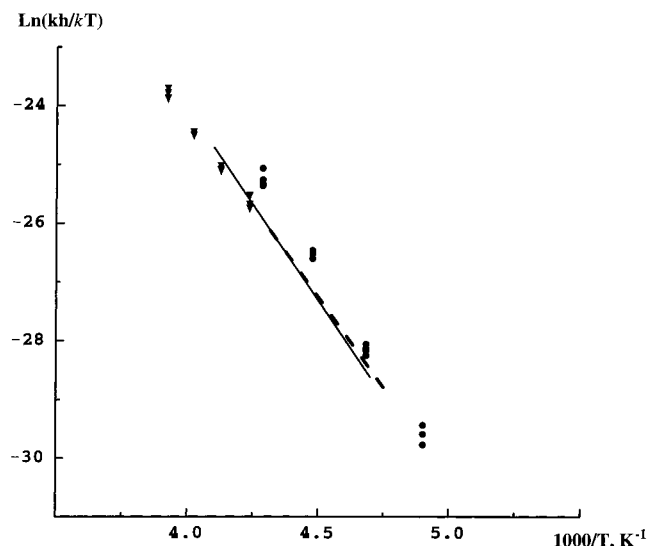


Figure 4. Comparative Eyring plot of activation parameters of the cyclic exchange in $[(\text{TMP})\text{Fe}(2\text{-MeImH})_2]^+$ obtained in this and previous studies: \blacktriangledown , this work; dashed line, ref 2; \bullet , ref 4; solid line, ref 5.

as the T_2 (this work), measurements of the rate constant of the cyclic exchange in $[(\text{TMP})\text{Fe}(2\text{-MeImH})_2]^+$.

A comparative plot of the exchange rate constants obtained in this and previous²⁻⁵ studies is shown in Figure 4. The thermodynamic activation parameters of the exchange are summarized in Table 1. From these, it is evident that the results of all of the experimental measurements are in a good general agreement: considering the error of the determination of the activation parameters, the activation entropy of the cyclic exchange is zero and the activation enthalpy is 50 kJ/mol. The only exceptions from this statement are the activation parameters obtained from the ST measurements.⁴

It is evident from Figure 4 that the ST measurements systematically overestimate the value of the exchange rate constant. One of the reasons for this may be the presence of spin diffusion during the 5 s irradiation period in the ST experiments. Indeed, spin diffusion may cause the presence of channels of magnetization transfer that are not accounted for in eqs 1-4 in ref 4 used in the derivation of peak intensities in ST experiments. These additional channels would compliment the exchange rate matrix (eq 5, this paper). Therefore, the existence of the steady state in ST experiments is not in itself sufficient evidence that the measured magnetizations are those created exclusively by the cyclic exchange. Nevertheless, the presence of spin diffusion in the studied system is a speculative assumption and should not be considered a conclusion of this study.

From the point of view of statistical thermodynamics, the zero activation entropy of the cyclic exchange in $[(\text{TMP})\text{Fe}(2\text{-MeImH})_2]^+$ is not obvious. A positive activation entropy is likely to be the consequence of the increased accessibility of vibrational and internal rotational degrees of freedom in the activated complex. The activation of the chemical exchange between the pyrrole protons has to be accompanied by the removal of the ruffling of the metalloporphyrin core.⁴ Such a deformation can unfreeze the internal rotation of axial ligands, which would mean a positive contribution to the activation entropy.

Another reason for the possible existence of a nonzero activation entropy may be associated with the reorganization of the solvent that accompanies the change of the complex geometry. Preliminary measurements indicate that ΔH^\ddagger in

$[(\text{TMP})\text{Fe}(1,2\text{-Me}_2\text{Im})_2]^+$ may be as low as 40 kJ/mol. This complex is different from $[(\text{TMP})\text{Fe}(2\text{-MeImH})_2]^+$ only in that it contains two additional methyl groups that face the solvent and eliminate the possibility of hydrogen-bond donation from the imidazole N_1H to the solvent and the ion-paired anion. In vacuo molecular mechanics studies of both complexes result in identical equilibrium structures and barriers of ligand rotation.⁴ The presence of such a significant difference in the ΔH^\ddagger values of the two complexes probably indicates the presence of a significant solvent effect on the axial ligand rotation, which is likely the result of the difference in interaction of polar solvent molecules (CD_2Cl_2) with the $\text{N}_1\text{-R}$ moiety of the 1,2-dimethylimidazole ligand and the hydrogen-bonding interactions of the $\text{N}_1\text{-H}$ moiety of the 2-methylimidazole ligand. Such interaction should be expected to be greater for the $\text{N}_1\text{-H}$ case than for N-substituted imidazoles because of the higher polarity of the N-H bond and the partial deprotonation of the imidazole ligand because of the hydrogen bonding to the associated anion.³⁹ Through this effect, solvent reorganization around the activated complex could contribute to making the activation entropy different for the 1,2-dimethylimidazole than the 2-methylimidazole complex.

The rates of axial ligand rotation in the analogous $[(\text{TMP})\text{Co}(2\text{-MeImH})_2]^+$ complex and its bis(1,2- Me_2Im) analogue have been studied by EXSY techniques and found to have ΔH^\ddagger (48.1 and 43.9 kJ/mol, respectively) fairly similar to the respective Fe(III) complexes but very negative ΔS^\ddagger (-62 and -84 J/K \cdot mol, respectively).² Besides the slightly shorter bond lengths (~ 0.05 Å)⁴⁰ of Co(III) porphyrinates, the anion used in the Co(III) complex was BF_4^- , which is slightly smaller than ClO_4^- and may induce tighter solvation of the Co(III) complexes. Either or both factors may be responsible for the large, negative entropies of activation for the Co(III) analogues. In any case, it is likely that solvation effects are important in determining the ΔS^\ddagger of axial ligand rotation.

Despite differences in the activation entropy between the Fe(III) and Co(III) complexes, it is the conclusion of this paper that the activation entropy in the studied complex, $[(\text{TMP})\text{Fe}(2\text{-MeImH})_2]^+$, is close to the experimental error, which can be estimated as approximately 6 J/K \cdot mol.

Acknowledgment. The support of this work by the National Institutes of Health [Grant DK 31038 (F.A.W.)], the Materials Characterization Program at the University of Arizona, and the Department of Chemistry for a Mid-Career Scholarship (K.I.M.) is gratefully acknowledged.

References and Notes

- (1) Present address: Department of Chemistry, CB #3290, University of North Carolina, Chapel Hill, NC 27599-3290.
- (2) Shokhirev, N. V.; Shokhireva, T. Kh.; Polam, J. R.; Watson, C. T.; Raffii, K.; Simonis, U.; Walker, F. A. *J. Phys. Chem.* **1997**, *101*, 2778.
- (3) Polam, J. R.; Shokhireva, T. Kh.; Raffii, K.; Simonis, U.; Walker, F. A. *Inorg. Chim. Acta* **1997**, *263*, 109.
- (4) Momot, K. I.; Walker, F. A. *J. Phys. Chem. A* **1997**, *101*, 2787.
- (5) Nakamura, M.; Groves, J. T. *Tetrahedron* **1988**, *44*, 3225.
- (6) Nakamura, M.; Tajima, K.; Tada, K.; Ishizu, K.; Nakamura, N. *Inorg. Chim. Acta* **1994**, *224*, 113.
- (7) Munro, O. Q.; Marques, H. M.; Debrunner, P. G.; Mohanrao, K.; Scheidt, W. R. *J. Am. Chem. Soc.* **1995**, *117*, 935.
- (8) Momot, K. I.; Walker, F. A. *J. Phys. Chem. A* **1997**, *101*, 9207.
- (9) Sandström, J. *Dynamic NMR Spectroscopy*; Academic Press: New York, 1982.
- (10) (a) Allerhand, A.; Gutowsky, H. S. *J. Chem. Phys.* **1964**, *41*, 2115.
- (b) Allerhand, A.; Gutowsky, H. S. *J. Chem. Phys.* **1965**, *42*, 1587.
- (11) Hahn, E. L. *Phys. Rev.* **1950**, *80*, 580.

- (12) (a) *Mathematica*, version 2.2 for the X Window System; Wolfram Research, Inc.: Champaign, IL, 1993. (b) Wolfram, S. *The Mathematica Book*; Wolfram Media: Champaign, IL; Cambridge University Press: Cambridge, 1996.
- (13) Güntert, P.; Schaefer, N.; Otting, G.; Wüthrich, K. *J. Magn. Reson. A* **1993**, *101*, 103.
- (14) Shriver, J. W. *J. Magn. Reson.* **1991**, *94*, 612.
- (15) (a) Nessel, M. J. M. Ph.D. Thesis, University of Arizona, Tucson, AZ, 1994. (b) Nessel, M. J. M.; Shokhirev, N. V.; Enemark, P. D.; Jacobson, S. E.; Walker, F. A. *Inorg. Chem.* **1996**, *35*, 5188.
- (16) (a) *Felix 95.0 NMR Data Processing, Analysis and Assignment: Command Language Guide*; Biosym/Molecular Simulations: San Diego, 1995. (b) *Felix 95.0 NMR Data Processing, Analysis and Assignment: Tutorials*; Biosym/Molecular Simulations: San Diego, 1995.
- (17) Korn, G. A.; Korn, T. M. *Mathematical Handbook for Scientists and Engineers*, 2nd ed.; McGraw-Hill: New York, 1968.
- (18) Bevington, P. R. *Data Reduction and Error Analysis for the Physical Sciences*; McGraw-Hill: New York, 1969.
- (19) Slichter, C. P. *Principles of Magnetic Resonance*, 3rd ed.; Springer-Verlag: New York, 1990.
- (20) Jen, J. *J. Magn. Reson.* **1981**, *45*, 257.
- (21) Dimitrov, V. S.; Ladd, J. A. *J. Magn. Reson.* **1979**, *36*, 401.
- (22) Vasavada, K. V.; Kaplan, J. I. *J. Magn. Reson.* **1985**, *62*, 37.
- (23) Reeves, L. W.; Shaw, K. N. *Can. J. Chem.* **1970**, *48*, 3641.
- (24) Schotland, J.; Leigh, J. S. *J. Magn. Reson.* **1983**, *51*, 48.
- (25) Rabinovitz, M.; Pines, A. *J. Am. Chem. Soc.* **1969**, *91*, 1585.
- (26) Allan, E. A.; Hobson, R. F.; Reeves, L. W.; Shaw, K. N. *J. Am. Chem. Soc.* **1972**, *94*, 6604.
- (27) Bushweller, C. H.; Bhat, G.; Letendre, L. J.; Brunelle, J. A.; Bilofsky, H. S.; Ruben, H.; Templeton, D. H.; Zalkin, A. *J. Am. Chem. Soc.* **1975**, *97*, 65.
- (28) Campbell, I. D.; Dobson, C. M.; Ratcliffe, R. G.; Williams, R. J. P. *J. Magn. Reson.* **1978**, *29*, 397.
- (29) Dimitrov, V. S.; Vassilev, N. G. *Magn. Reson. Chem.* **1995**, *33*, 739.
- (30) Bain, A. D.; Cramer, J. A. *J. Magn. Reson. A* **1996**, *118*, 21.
- (31) *Dynamic Nuclear Magnetic Resonance Spectroscopy*; Jackman, L. M., Cotton, F. A., Eds.; Academic Press: New York, 1975.
- (32) Steigel, A. Mechanistic Studies of Rearrangements and Exchange Reactions by Dynamic NMR Spectroscopy. In *Dynamic NMR Spectroscopy*; Diehl, P., Fluck, E., Kosfeld, R., Eds.; Springer-Verlag: New York, 1978.
- (33) Higgins, T. B.; Safo, M. K.; Scheidt, W. R. *Inorg. Chim. Acta* **1990**, *178*, 261.
- (34) Walker, F. A.; Simonis, U. *J. Am. Chem. Soc.* **1991**, *113*, 8652.
- (35) Luz, Z.; Meiboom, S. *J. Chem. Phys.* **1964**, *40*, 1058.
- (36) Satterlee, J. D.; La Mar, G. N.; Bold, T. J. *J. Am. Chem. Soc.* **1977**, *99*, 1088.
- (37) La Mar, G. N.; Walker, F. A. *J. Am. Chem. Soc.* **1972**, *94*, 8607.
- (38) Perrin, C. L. *J. Magn. Reson.* **1989**, *82*, 619.
- (39) Chacko, V. P.; La Mar, G. N. *J. Am. Chem. Soc.* **1982**, *104*, 7002.
- (40) Scheidt, W. R.; Lee, Y. J. *Struct. Bonding (Berlin)* **1987**, *64*, 1.